Society For Biomaterials

Design and optimization of biocompatible polycaprolactone/poly (L-lactic-*co*-glycolic acid) scaffolds with and without microgrooves for tissue engineering applications

Cristhiane Alvim Valente,[1] Pedro Cesar Chagastelles,[2,3] Natália Fontana Nicoletti,[2,3] Giovanna Ramos Garcez,[1] Bruna Sgarioni,[4] Fábio Herrmann,[5] Gustavo Pesenatto,[5] Eduardo Goldani,[2,3] Mara Lise Zanini,[4] Maria Martha Campos,[3] Ricardo Meurer Papaléo,[1,6,7] Jefferson Braga da Silva,[2,5] Nara Regina de Souza Basso[1,4,7]

[1]Graduate Program in Materials Engineering and Technology, Pontifícia Universidade Católica do Rio Grande do Sul, Porto Alegre, RS, Brazil
[2]Graduate Program in Medicine and Health Sciences, Pontifícia Universidade Católica do Rio Grande do Sul, Porto Alegre, RS, Brazil
[3]Institute of Toxicology and Pharmacology, Pontifícia Universidade Católica do Rio Grande do Sul, Porto Alegre, RS, Brazil
[4]Faculty of Chemistry, Pontifícia Universidade Católica do Rio Grande do Sul, Porto Alegre, RS, Brazil
[5]Faculty of Medicine, Pontifícia Universidade Católica do Rio Grande do Sul, Porto Alegre, RS, Brazil
[6]Faculty of Physics, Pontifícia Universidade Católica do Rio Grande do Sul, Porto Alegre, RS, Brazil
[7]Interdisciplinary Center of Nanoscience and Micro-nanotechnology, Pontifícia Universidade Católica do Rio Grande do Sul, Porto Alegre, RS, Brazil

Received 17 July 2017; revised 4 January 2018; accepted 24 January 2018
Published online 16 February 2018 in Wiley Online Library (wileyonlinelibrary.com). DOI: 10.1002/jbm.a.36355

Abstract: This study investigated the effects of smooth and microgrooved membrane blends, with different polycaprolactone (PCL)/ poly(lactic-*co*-glycolic acid) (PLGA) ratios on the viability, proliferation, and adhesion of different mammalian cell types. The polymer matrices with and without microgrooves, obtained by solvent casting, were characterized by field-emission scanning electron microscopy, atomic force microscopy, contact angle and Young's modulus. Blend characterization showed an increase in roughness and stiffness of membranes with 30% PLGA, without any effect on the contact angle value. Pure PCL significantly decreased the viability of Vero, HaCaT, RAW 264.7, and human fetal lung and gingival fibroblast cells, whereas addition of increasing concentrations of PLGA led to a reduced cytotoxicity. Increased proliferation rates were observed for all cell lines. Fibroblasts adhered efficiently to smooth membranes of the PCL70/PLGA30 blend and pure PLGA, compared to pure PCL and silicone. Microgrooved membranes promoted similar cell adhesion for all groups. Microstructured membranes (15 and 20-μm wide grooves) promoted suitable orientation of fibroblasts in both PCL70/PLGA30 and pure PLGA, as compared to pure PCL. Neuronal cells of the dorsal root ganglion exhibited an oriented adhesion to all the tested microgrooved membranes. Data suggest a satisfactory safety profile for the microgrooved PCL70/PLGA30 blend, pointing out this polymer combination as a promising biomaterial for peripheral nerve regeneration when cell orientation is required. © 2018 Wiley Periodicals, Inc. J Biomed Mater Res Part A: 106A: 1522–1534, 2018.

Key Words: PCL, PLGA, blend, orientation, microgrooves

How to cite this article: Alvim Valente C, Cesar Chagastelles P, Fontana Nicoletti N, Ramos Garcez G, Sgarioni B, Herrmann F, Pesenatto G, Goldani E, Zanini ML, Campos MM, Meurer Papaléo R, Braga da Silva J, de Souza Basso NR. 2018. Design and optimization of biocompatible polycaprolactone/poly(L-lactic-*co*-glycolic acid) scaffolds with and without microgrooves for tissue engineering applications. J Biomed Mater Res Part A 2018:106A:1522–1534.

INTRODUCTION

The development of multifunctional biomaterials for tissue engineering applications has focused on improving their therapeutic properties to overcome many of the clinical issues related to loss of function of organs and tissues, such as peripheral nerves, bones, muscles, and tendons.[1–3] Different biomaterials are available for clinical applications;[2,4–6] however, serious injury with an extensive tissue loss benefits exclusively from tissue or organ transplantation, as no artificial therapy has been satisfactorily developed for this end up to now.[2] Therefore, current research efforts are focused to improve biomaterial-driven tissue

Correspondence to: N. R. de Souza Basso; e-mail: nrbass@pucrs.br
Contract grant sponsor: Conselho Nacional de Desenvolvimento Científico e Tecnológico (CNPq)
Contract grant sponsor: Coordenação de Aperfeiçoamento de Pessoal de Nível Superior (CAPES)
Contract grant sponsor: Institutional grant (PRAIAS)

regeneration[7] in response to the demand for new tissues and organs for clinical applications.[1,2,6]

Strategies to improve biomaterial characteristics include the combination of different natural and/or synthetic polymers, the composition of polymer mixtures, the use of nano- and microstructuration, as well as chemical modification of surfaces, aiming to obtain multifunctional materials or multihybrid systems that gather biocompatibility, mechanical, and structural properties[1,2,7–10] and biomaterial-driven regeneration.[6,8,11]Several polymers, copolymers, and blends are used to produce biomaterials such as polycaprolactone (PCL) and poly(lactic-*co*-glycolic acid) (PLGA). These are biodegradable polymers approved by the Food and Drug Administration (FDA) for clinical use.[2,5,8,12] PLGA is one of the most widely used biodegradable polymers in scaffold preparation for tissue engineering owing to its easy manufacturing, low inflammatory response and adjustability of degradation rates.[5] The degradation time can be modulated by tuning the ratio of its hydrophilic (polyglycolic acid) and hydrophobic (polylactic acid) constituents. PLGA with a high content of hydrophilic units show faster degradation process; that is, degradation of PLGA 50:50 (2–4 weeks) is fastest followed by PLGA 70:30 (6–8 weeks) and PLGA 85:15 (23–26 weeks).[13,14] PCL is another commonly employed polyester for tissue regeneration applications. Compared to PLGA, PCL is more flexible, less expensive and has low toxicity during the degradation process. The main disadvantages are relatively slow degradation rate (2–4 years), not suitable for devices used in short-term therapeutic applications, besides presenting a poor cellular adhesion.[14]

PLGA-based biomaterials with nano/microporous allow nutrient permeability and favor cell adhesion and proliferation.[9,12,15,16] PCL presents good mechanical proprieties and has been used in blends with other biocompatible polymers to counterbalance biological and mechanical features.[1,17] Blends of PCL and PLGA are used to control cell adhesion and to adjust degradation time.[1,10,18–20]

Both *in vitro* and *in vivo* experimental evidence demonstrated that biomaterials with nano- and/or microstructures on their surface significantly influence cell behavior such as adhesion, morphology, and migration.[1,21–24] The surface roughness of scaffolds is an important characteristic involved in cell biocompatibility, and several studies correlate rougher surfaces with increased cell affinity to materials.[25,26] For instance, axonal growth occurs longitudinally to the nerve fibers, and this orientation is essential for an efficient nerve regeneration. One strategy to promote cell guidance is the creation of longitudinal grooves in the internal surface of conduits.[27] Studies have explored the role of microgrooved membranes on cell shape and orientation.[22,23,27–30] These patterned surfaces can favor the alignment, elongation, and polarization of Schwann cells,[23,29–31] neural cell lines,[27] dorsal root ganglia cells[32] and adipose-derived mesenchymal stem cells,[22] when compared to smooth surfaces.

The present study aimed at evaluating the effects of microgrooved polymer blends composed by PCL/PLGA, on the toxicity, viability, proliferation, adhesion, and orientation of mammalian cells, providing new insights on the biocompatibility of this polymer mixture.

MATERIALS AND METHODS

All the chemicals used were of high purity, with analytical grade. PCL (molecular weight [Mn] = 80 000 g/mol) and phosphate buffered saline (PBS; 10× concentrate, suitable for cell culture, pH = 7.4) were supplied by Sigma-Aldrich company. Poly(L-lactic-*co*-glycolic acid) (PLGA; Purasorb PLG8523 [85/15] L-lactide/glycolide copolymer; inherent viscosity = 2.38 dL/g in chloroform) was supplied by Corbion Purac (Gorinchem, The Netherlands). Organic solvents such as chloroform were from Synth (Diadema, SP, Brazil). Deionized water was obtained from a Milli-Q water purification system (Millipore, Bedford, MA).

Preparation of smooth and microgrooved membranes

To obtain smooth membranes, pure PCL, pure PLGA, or mixtures of both polymers prepared at different PCL:PLGA ratios (90:10, 80:20, 70:30 w/w), were solubilized in chloroform, so that the final proportion of all solutions was 5% w/v. Solutions were poured in glass Petri-dishes at 0.5 mL/cm^2. The solutions were dissolved under an ultrasonic bath (40 kHz, Unique, USC-1600 model) for 4 h, and subsequently poured into a glass Petri-dish (5.5-cm in diameter). The solvent was evaporated at room temperature for 48 h. Subsequently, the membranes were vacuum-dried for 8 h. Microgrooved membranes were obtained using the same methodology described for smooth membrane; however, the solutions were poured on microstructured silicon molds. The molds were manufactured by photolithography on the *Centre Inter-Universitaire de Recherche et d'Ingénierie des Matériaux* (Toulouse, France) from *École Polytechnique Fédérale de Lausanne*. The molds were composed of parallel microgrooves of different widths (15 or 20 μm), with a fixed height of 25 μm, distributed in the shape of a rectangle of 0.9 × 1.2 mm.

Membrane degradation

The degradation experiments were carried out based on ASTM F1635-11 (2011).[33] The samples were cut into 5-mm diameter disks, and incubated at 37°C temperature and 60 rpm-stirring, in tubes containing 5 mL of PBS solution. Each batch contained three specimens for each incubation time. The specimens were removed from PBS solution after 7, 14, 28 and 90 days. They were carefully washed with deionized water, vacuum-dried to a constant weight, and then weighed to determine the mass loss (in mg). The percentages of mass loss were calculated from the following Eq. (1):

$$\text{Mass loss } (\%) = 100 \times (M_0 - M_t)/M_{0-}, \quad (1)$$

where M_0 is the mass before degradation and M_t is the dry mass after each time of degradation. Additionally, the pH of the removed PBS was measured after each time of degradation, in a pH-meter (Digimed, DM-20 model). The presented

values represent the average of three specimens ± standard deviation.

Membrane characterization

Atomic force microscopy. The atomic force microscopy (AFM) was used to collect for nanotopography and surface roughness data of membranes. The analyses were performed in the peak force tapping mode, using a Bruker Dimension Icon PT equipped with a TAP150A probe (Bruker, resonance frequency of 150 kHz and 5 N/m spring constant). The scanned area of the images was 30 × 30 μm with a sampling density of 512 lines per area. AFM images and the roughness measurements (Ra, Rq, and Rmax) were determined using the NanoScope Analysis software. The values were expressed as the average of three trials with standard deviation.

Scanning electron microscopy. The morphology of membranes was examined using field-emission scanning electron microscopy (SEM; FEI-Inspect F50 instrument). The surface morphology of smooth and microstructured membranes was compared. All samples were coated with a thin layer of gold.

Mechanical properties (Young's modulus). The mechanical properties of the membranes were measured using a Universal test machine (Lloyd Instruments, model LR5K Plus) equipped with holders for thin films (25 mm in width) at a distance of 600 mm and a load cell of 500 N. The speed of testing was 50 mm/min at room temperature in accordance with ASTM standard D882-12 (2012).[34].

Contact-angle measurement. The static water contact angle measurements were performed using a goniometer (Phoenix 300, SEO). All images were captured 5 s after the water droplets touched the sample surface in order to achieve measurements from unchanged sessile water droplets. Three drops of deionized water were applied to each membrane and the mean of the angles was calculated, considering an experimental error of 2° among the measurements. Reported values are averages ± standard deviation of at least three measurements taken at different points on the surface.

General cell culture protocols

VERO (kidney epithelial cells African green monkey), RAW 264.7 (mouse macrophage-like cells), HaCaT (human keratinocytes) or MRC-5 and HGF (human fetal lung and gingival fibroblast-like cells, respectively) cell lines were from American Type Culture Collection (ATCC-Rockville, MD). The cells were cultured in Dulbecco's Modified Eagle Medium with 10% fetal bovine serum, 100 U/ml penicillin and 100 μg/ml streptomycin, at a temperature of 37°C, a minimum relative humidity of 95%, and an atmosphere of 5% CO_2 in air. Polymeric membranes were disinfected with 1 mL of 70% ethanol for 3 min, and exposed to germicidal ultraviolet light for 30 min each side, in a class II safety cabinet. The cell lines were preseeded at 4×10^3 cells per well in 96-well plates for 3–(4,5-dimethylthiazol-2-yl)-2,5-diphenyltetrazolium bromide (MTT) and mitotic index analysis. They were seeded at 20×10^3 cells on the top of the membranes in 24-well plates for all other analyses. All experiments were performed in triplicate and repeated three times.

Isolation and culture of dorsal root ganglia cells

Cells of the dorsal root ganglia (DRG) were dissected from male Wistar rats (4–6 week-old, 180–200 g) after euthanasia by an overdose of inhaled sevoflurane. The spinal cord was surgically exposed and the ganglia were manually isolated and transferred to Dulbecco's Modified Eagle's Medium, supplemented with 10% fetal bovine serum, 100 U/ml penicillin and 100 μg/ml streptomycin. At least 16 ganglia were isolated per rat. After washing with PBS, the ganglia were digested with 1 mg/ml type 1 collagenase (Sigma-Aldrich) for 40 min at 37° C, followed centrifugation at 900 rpm for 10 min and an additional digestion step with 0.1% trypsin-EDTA solution for 15 min at 37° C. Then, the cells were transferred to a 15 mL conical tube with 5 mL of DMEM medium containing 10% of fetal bovine serum. Additional dissociation was performed mechanically using a sterile plastic Pasteur pipette. Cells were centrifuged at 900 rpm for 10 min. The pellet was resuspended in Neurobasal medium supplemented with 2% B27 and 100 ng/ml nerve growth factor-7 S (ThermoFisher Scientific), containing 100 U/ml penicillin, 100 μg/ml streptomycin, and 0.45 μg/mL gentamicin sulfate. Cells were plated on the surface of 15- and 20-μm microgrooved membranes or glass coverslips previously treated with Geltrex™ (ThermoFisher) according to manufacturer's instructions, in wells of a 24-well plate. Geltrex is a laminin-rich matrix used to facilitate cell attachment. DRG cells were cultured for 3 days with medium change every 24 h after plating, and they were subsequently immunostained with B-III-tubulin antibody.

Functional effects of polymeric matrices incubation

The cell lines were incubated with smooth or microgrooved membranes, prepared from the biodegradable polymers, pure or in blends, for 24 h. Blends of PCL/PLGA were prepared and tested at different proportions: PCL90/PLGA10, PCL80/PLGA20 and PCL70/PLGA30. PCL or PLGA were evaluated separately for comparison purposes. Silicone samples were used as a control of toxicity in some experiments. The polymers were incubated by direct contact at 6 cm^2/mL, as recommended by ISO 10993 (2009)[35] for the biological evaluation of sterile medical devices that come into direct or indirect contact with the human body.

Cell viability

The number of metabolically active cells was determined based on the mitochondrial reduction of a tetrazolium bromide salt (MTT assay), as an indicative of cell viability. The cells were incubated with different smooth and microgrooved membranes for 24 h, as described above. The results are expressed as the percentage of cell viability in relation to tissue-culture plate (smooth membranes) or pure PCL (microgrooved membranes).

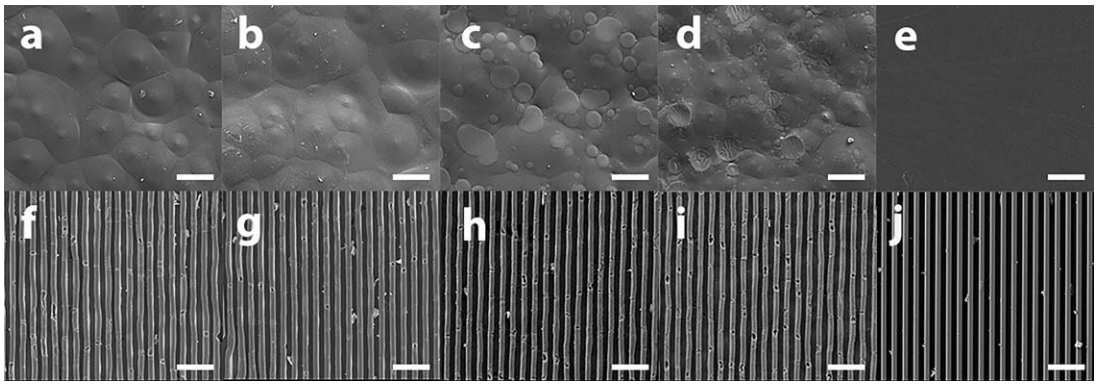

FIGURE 1. Microtopography of smooth and microgrooved membranes. SEM images: (a) pure PCL, (b) PCL90/PLGA10, (c) PCL80/PLGA20, (d) PCL70/PLGA30, and (e) pure PLGA smooth membranes and (f) pure PCL, (g) PCL90/PLGA10, (h) PCL80/PLGA20 (i) PCL70/PLGA30 blend, and (j) pure PLGA, all 15-μm microgrooved membranes. Original magnification ×500.

Nuclear morphology and mitotic index

The 4′,6-diamino-2-phenylindole (DAPI) staining was carried out to establish the mitotic index as a parameter of cell proliferation. Briefly, the cells were seeded in 24- and 96-well plates and incubated with the polymer membranes for 24 h. After incubation, the cells were washed three times in PBS, and fixed with 4% formaldehyde at room temperature, for 15 min. The fixed cells were then washed with PBS, permeabilized with 0.1% Triton X-100 in PBS and stained with a 300 n*M* DAPI solution (Santa Cruz, CA) at room temperature, for 10 min. The nuclear morphology of the cells was examined under a fluorescent microscope (Carl Zeiss MicroImaging GmbH, Germany). DAPI staining clearly delineates mitotic figures, and it is possible to determine the mitotic index for each automatic cell count. The mitotic index was calculated as the number of mitotic events in 10 fields per well, three times in triplicate.

Assessment of live and dead cells

The HGF, MRC-5 or RAW 264.7 cell lines were plated at 5×10^4 cells/well on the surface of silicone, pure PLGA, pure PCL or the blend PCL70/PLGA30 and cultured for 24 or 72 h. The analysis of living and dead cells was carried out by using fluorescein diacetate and propidium iodide (PI), respectively. Briefly, the cells were incubated for 30 min with 8 μg/mL fluorescein diacetate and 5 μg/mL PI in DMEM. Then, the cells were analyzed by fluorescence microscopy (Olympus). Fluorescent images were taken to qualitatively assess the cell viability and adhesion.

Morphology and cell distribution on the membranes

The HGF, MRC-5, and RAW 264.7 cell lines were plated at 5×10^4 cells/well on the surface of silicone, pure PLGA, or PCL70/PLGA30, and cultured for 24 or 72 h. The cells were fixed for 30 min with 4% paraformaldehyde (PFA), and sequentially dehydrated in increasing concentrations of ethanol (50, 70, 85, 95, and 100%), for 30 min each. The samples were left for 1 h in 100% ethanol, and allowed to air dry at room temperature. The analysis of cell morphology was assessed by SEM with accelerating voltage of 10 kV, using a sputter coater (Bal-Tec SCD 050) after coating with a thin layer of gold.

Cell orientation on microgrooved membranes

Initially, to evaluate the capacity of cell orientation, we chose the fibroblast cell lines MRC-5 and HGF, which were cultured on the surface of microgrooved membranes. The orientation angle of the cells was represented by the orientation order parameter S, defined as $S = <3\cos\theta^2 - 1>/2$, where θ is the angle that cells assume, relative to the angle measured for the membrane groves. Cells randomly distributed present S values close to zero, whereas cells with a parallel orientation present values close to 1.[36] The angles were manually determined by using NIH ImageJ 1.36b Software. Sixty measurements per image were taken from three different regions of a membrane.

Next, the capacity of orientation of neurons was qualitatively assessed by culturing DRG cells on 15- or 20-μm microgrooved membranes or glass coverslips, previsouly treated with Geltrex according to manufacter's instructions. After 3 days, the cells were fixed in 4% PFA for 30 min and washed three times with PBS. Cells were blocked and permeabilized with PBS solution containing 1% BSA and 0.1% Triton X-100 for 30 min at room temperature. Then, cells were incubated with a mouse anti-B-III-tubulin antibody for 2 h at 37° C (T8578, Sigma-Aldrich diluted 1:500) to identify neurons. The corresponding Alexa 555-conjugated secondary antibody (Invitrogen, Carlsbad, CA, diluted 1:500) and DAPI (Invitrogen, Carlsbad, CA) were added to visualize the cells. Images were obtained in a fluorescence microscope (Olympus).

Statistical analyses

The number of experimental replications is provided in the figure legends. Data were analyzed by one-way (ANOVA) followed by Tukey's *post hoc* test, using SPSS® software or Graph-Pad software (San Diego, CA). $p < 0.05$ was indicative of statistical significance.

RESULTS

Surface characterization, Young's modulus and *in vitro* mass loss behavior of the membranes

Figure 1 shows the SEM images of the membrane surfaces prepared by solvent casting. The presence of spherical aggregations (dome-like domains) was observed on the

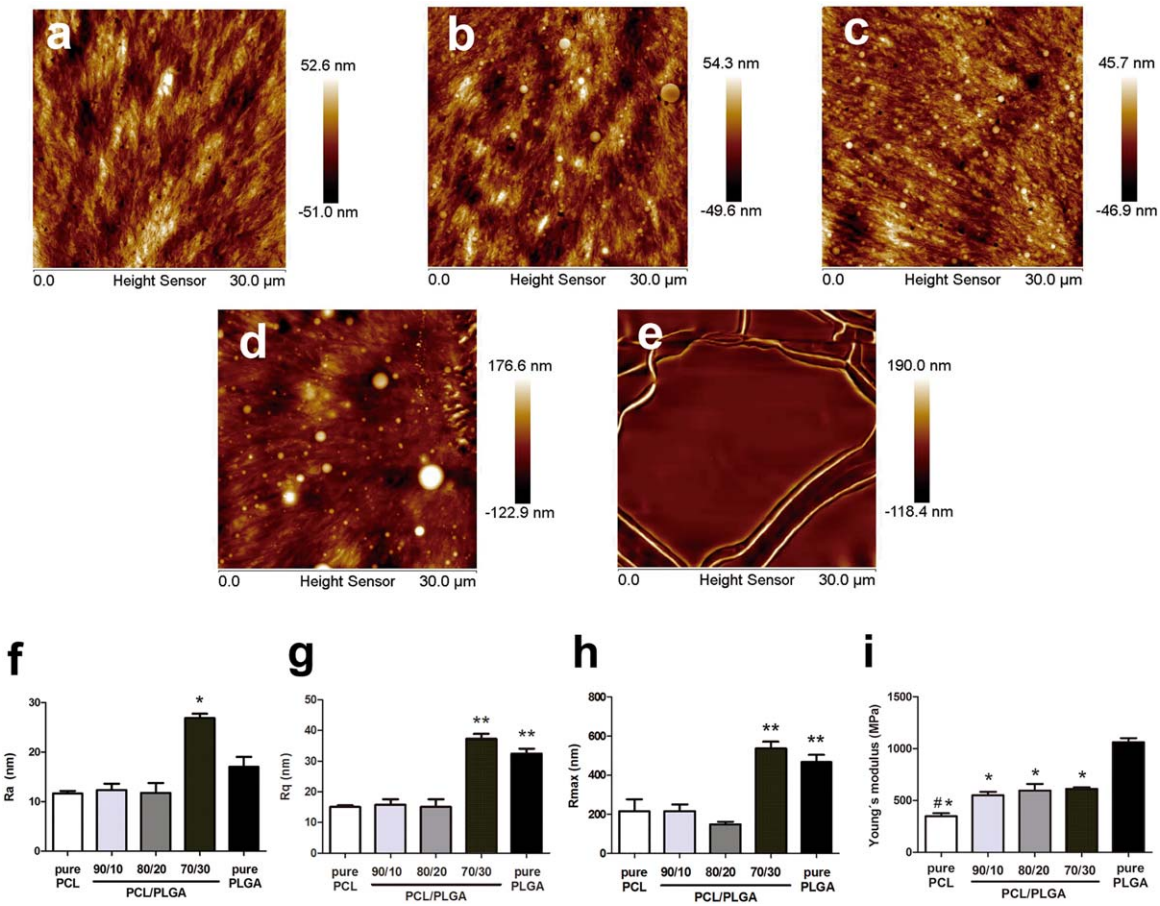

FIGURE 2. 2D AFM images of smooth membranes varying the PCL to PLGA ratio: (a) pure PCL, (b) PCL90/PLGA10, (c) PCL80/PLGA20, (d) PCL70/PLGA30, and (e) pure PLGA. Surface roughness parameters (30 μm^2 scan size): (f) average roughness (Ra); (g) root-mean-square roughness (Rq) and (h) maximum roughness height (Rmax). Analysis made on the surface of the membrane that remained in contact with the air (upper surface). $*p < 0.0001$ versus all other groups, $**p < 0.0001$ versus pure PCL, 90/10 and 80/20. One-way ANOVA followed by Tukey *post hoc* test; (i) Young's modulus of smooth membranes. The Young's modulus were affected by PLGA incorporation in all PCL/PLGA membranes. $*p < 0.0001$ vs. pure PCL, $\#p < 0.05$ versus all other groups, One-way ANOVA followed by Tukey *post hoc* test.

surface of pure PCL membranes [Fig. 1(a)], suggesting a crystalline organization.[19,37] In contrast, pure PLGA surface was flat, smooth and nonporous, with no evidence of surface irregularity [Fig. 1(e)]. The incorporation of PLGA in the blends dotting the surface with immiscible PLGA was more evident when the ratio between PCL/PLGA increased to 80/20 and 70/30 [Fig. 1(c,d)]. The microstructure altered significantly the surface morphology of membranes [Fig. 1(f–j)]. The grooves presented a longitudinal alignment, with an average width for all groups of 14.02 ± 0.87 and 19.28 ± 1.19-µm, which are close to the expected for the 15 and 20 µm molds, respectively [Fig. 1(f–j)]. No significant differences in groove width were observed among groups (data not shown).

Figure 2 shows the surface roughness of smooth membranes evaluated by AFM analysis. PLGA incorporation produces a rough surface on PCL70/PLGA30 [Fig. 2(d,f–h)] that is similar to pure PLGA [Fig. 2(e,f–h)] and higher than pure PCL [Fig. 2(a,f–h)] and the other blends. It was possible to observe regions of immiscibility of PLGA in the PCL matrix in all the blends [Fig. 2(b–d)]. Undulations were observed on the surface of all membranes, and higher amount of PLGA favored the changes in topography. Higher values of surface roughness parameters, such as average roughness (*Ra*), root-mean-square roughness (*Rq*), and maximum roughness height (Rmax) were observed for PCL70/PLGA30 membranes [Fig. 2(d,f–h)]. Furthermore, according to the results of Young's modulus, the addition of PLGA to PCL resulted in less flexible blends compared to pure PLGA, with no difference among the blends [Fig. 2(i)]. The Young's modulus for smooth membranes of pure PCL, PCL/PLGA (90/10, 80/20, 70/30) and pure PLGA were 348 ± 51, 549 ± 60, 596 ± 113, 612 ± 26, and 1062 ± 68 MPa, respectively [Fig. 2(i)].

An important aspect to consider about biodegradable polymers is the degradation process, since it affects the cell growth and tissue regeneration. PCL and PLGA have been known to degrade at different rates by simple hydrolysis of ester bonds. The degradation kinetics is affected by factors related to the physicochemical characteristics of the polymer system.[9,18,23,37–39] In this study, the effects of PCL:PLGA blending and microgrooving were investigated through

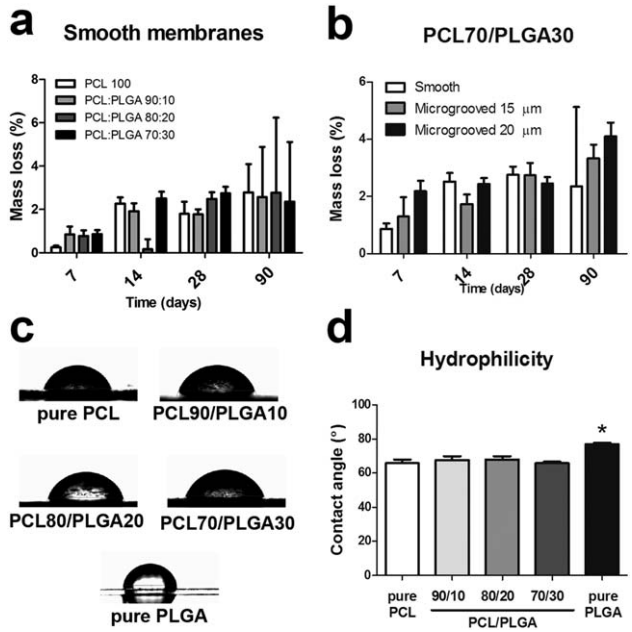

FIGURE 3. Percent of mass loss as a function of degradation time for (a) smooth membranes varying the PCL to PLGA ratio, and (b) smooth and microgrooved PCL70/PLGA30 blends. Two-way ANOVA followed by Tukey *post hoc* test, $p > 0.05$, $n = 3$. (c) Images of the drops formed on membrane surface for each group and (d) contact angle values. Analysis made on the surface of the membrane that remained in contact with the air. $^*p < 0.05$ versus all other groups, One-way ANOVA followed by Tukey *post hoc* test.

90 days of degradation, in an aqueous physiological environment, PBS [Fig. 3(a,b)]. The mass loss dynamics was slow and similar for all compositions, ranging from 0.5 to 7%. These data indicate no statistical difference in mass loss among the groups, neither for smooth [Fig. 3(a)] or microgrooved membranes [Fig. 3(b)], until 90 days of incubation. Furthermore, no significant changes were found in the pH of the incubation solution, throughout all the degradation period, remaining at approximately 7.4 (data not shown). Our study showed a good correlation between the low weight loss of all membranes and insignificant pH variations in the PBS solution, as shown in other studies with similar matrices and time.[37–40]

The surface hydrophobicity of the scaffolds is a relevant key factor for governing cell response, which can be assessed by measuring the contact angle through water spread of a droplet on the surface.[26] All smooth membranes indicated favorable hydrophilicity and exhibited water contact angles of $65.8 \pm 5.6°$ (pure PCL), $67.5 \pm 4.1°$ (PCL/PLGA 90:10), $67.9 \pm 3.1°$ (PCL/PLGA 80:20), $65.7 \pm 1.7°$ (PCL/PLGA 70:30) and $76.8 \pm 1.5°$ (pure PLGA). Contact angle measurements did not differ between pure PCL and the different blends, suggesting that the amount of PLGA used had no effect on membranes hydrophilicity [Fig. 3(c,d)]. The contact angle of pure PLGA membranes was slightly higher when compared to the other groups [Fig. 3(c,d)]. Despite these differences, all smooth membranes are considered hydrophilic; this might be advantageous for cell adhesion and tissue integration.

Biocompatibility of membranes

Cell viability. The effects of smooth membranes were initially evaluated by MTT assay in five distinct cell lineages. Pure PCL and the PCL90/PLGA10 blend caused a significant decrease in cell viability of VERO, RAW 264.7, and HaCaT cells. The maximal antiproliferative effect of neat PCL was observed in VERO cells [Fig. 4(a)], whereas the maximal reduction of cell viability with the PCL90/PLGA10 blend was seen in RAW 264.7 cells [Fig. 4(b)]. Pure PCL also triggered a significant decrease of HaCaT cell viability [Fig. 4(c)]. However, the tested polymers, alone or combined, did not significantly alter the viability of MRC-5 and HGF cells [Fig. 4(d,e)]. On the other hand, PCL80/PLGA20 and PCL70/PLGA30 blends did not display any cytotoxicity in all tested cell lines. The blends PCL80/PLGA20 and PCL70/PLGA30 were selected for further analysis using microgrooved membranes. Interestingly, the results found with microgrooved blends were similar to those obtained

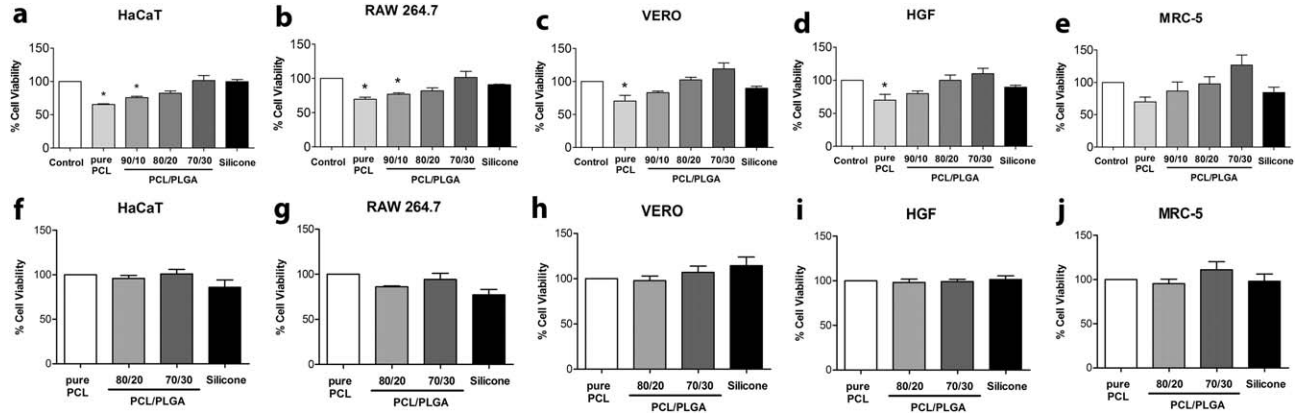

FIGURE 4. The metabolic activity was measured by MTT assay for (a,f) HaCaT, (b,g) RAW 264.7, (c,h) VERO, (d,i) HGF, and (e,j) MRC-5 cell lines after 24 h incubation with smooth (a–e) and microgrooved (f–j) membranes. Tissue-culture plate and silicone were used as controls for smooth membrane comparisons while pure PCL was used for the comparisons of microgrooved membranes. $^*p < 0.05$ versus control, One-way ANOVA with Tukey *post hoc* test, ($n = 3$).

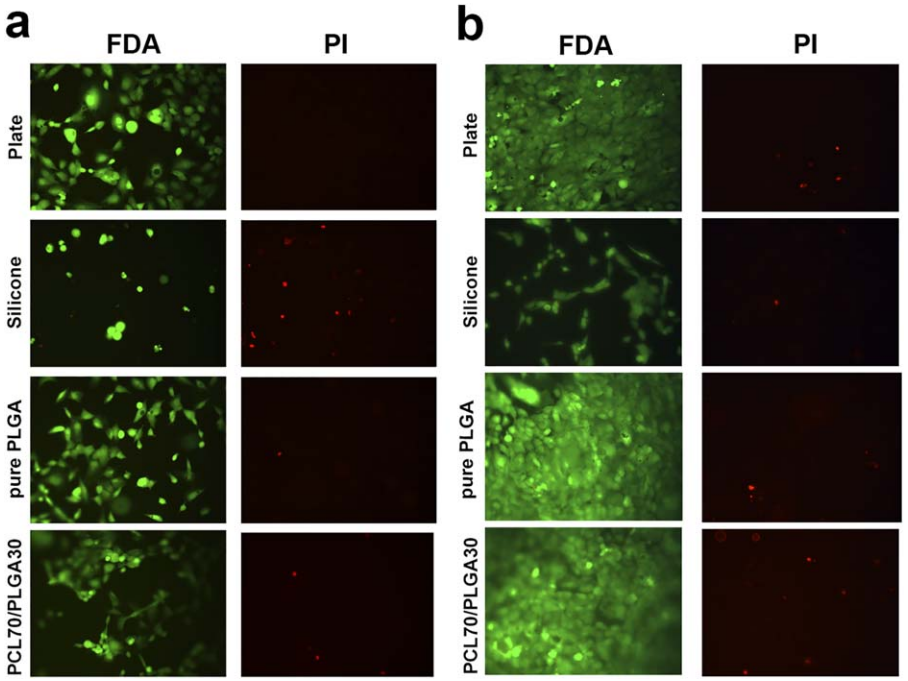

FIGURE 5. Fluorescence microscopy to assess the viability of fibroblast cells (HGF cell line). Representative images of living (green) and dead cells (red) cultured on tissue culture plates, silicone, smooth membranes of pure PLGA and PCL70/PLGA30 blend, after 24 (a) or 72 h (b). Original magnification ×100.

for smooth blends and no cytotoxicity was observed even for pure PCL [Fig. 4(f–j)].

Cell proliferation. To assess the proliferative cell profile in smooth membranes, the mitotic index was determined by DAPI staining. This set of experiments revealed that PCL alone markedly reduced the mitotic index in all the tested cell lines, as well as the blend PCL90/PLGA10 did [Fig. 5(a–e)]. Of note, the cells exposed to PCL70/PLGA30 showed a frequency of mitotic events similar to the negative control group [Fig. 5(a–e)]. Representative images of mitotic events are shown in Figure 5(f–h), confirming that cells cultured on tissue-culture plate and PCL70/PLGA30 blend showed a favorable proliferative profile compared to pure PCL [Fig. 5(h)].

Cell adhesion and orientation. Analysis of cell adhesion by fluorescence microscopy and SEM [Fig. 6(a,b)] showed that fibroblasts adhered to the surface of smooth pure PLGA membranes after 24 h [Fig. 6(a)] and remained attached for at least 72 h [Fig. 6(b)]. In contrast, smooth pure PCL membranes did not allow the efficient attachment of fibroblasts, as evidenced by SEM analysis (Fig. 7). The doping of PLGA to PCL (70/30) restored the capacity of fibroblasts adhesion and spread [Figs. 6(a,b) and 7]. Murine macrophages were able to adhere to all groups of smooth membranes (data no shown). The results from microgrooved membranes showed fibroblasts inside the grooves and attached to both sides of walls in 15- and 20-μm width grooves. Fibroblast morphology did not show apparent differences among microgrooved membrane groups (Fig. 7).

To verify the physical interaction between polymer blends and cells, the orientation of the cells in parallel microgrooved membranes was measured. After 72 h, HGF and MRC-5 cells attached to the polymer surface, elongated and arranged along both 15- and 20-μm membrane grooves (Fig. 8). The quantification of cell orientation was performed on fluorescein diacetate-stained cells. All membrane groups have orientation values that differ significantly from random tissue culture plate used as control [Fig. 8(m–p)]. Both cell lines presented high orientation indexes in pure PLGA group on 15 μm microgrooves (0.963 ± 0.02 for HGF and $0{,}981 \pm 0.004$ for MRC-5) and on 20 μm microgrooves (0.96 ± 0.006 for HGF and 0.97 ± 0.01 for MRC-5). The S index of PCL70/PGLA30 for 15 μm grooves was 0.95 ± 0.01 and 0.93 ± 0.01 for HGF and MRC-5, respectively, and for 20 μm was 0.92 ± 0.01 and 0.92 ± 0.01 for HGF and MRC-5, indicating that this blend preserves the capacity of cell orientation compared to pure PLGA [Fig. 8(o,p)]. The pure PCL group presented significantly lower S indexes compared to the other membrane groups (0.84 ± 0.03 for HGF and 0.81 ± 0.02 for MRC-5) on both 15- and (0.82 ± 0.004 for HGF and 0.84 ± 0.01 for MRC-5) 20-μm microgrooves [Fig. 8(o,p)]. Random orientations were observed for cells cultured on tissue culture plate (0.32 ± 0.04 for HGF and 0.35 ± 0.06 for MRC-5) [Fig. 8(m–p)]. No differences of cell orientation values were observed between 15 and 20 μm, inside each group. To assess the ability of nerve cells to adhere and orientate to the microgrooved membranes, we performed separate experiments with cells isolated from the dorsal root ganglia. After 72 h, it was possible to observe that all membranes promoted the guidance and

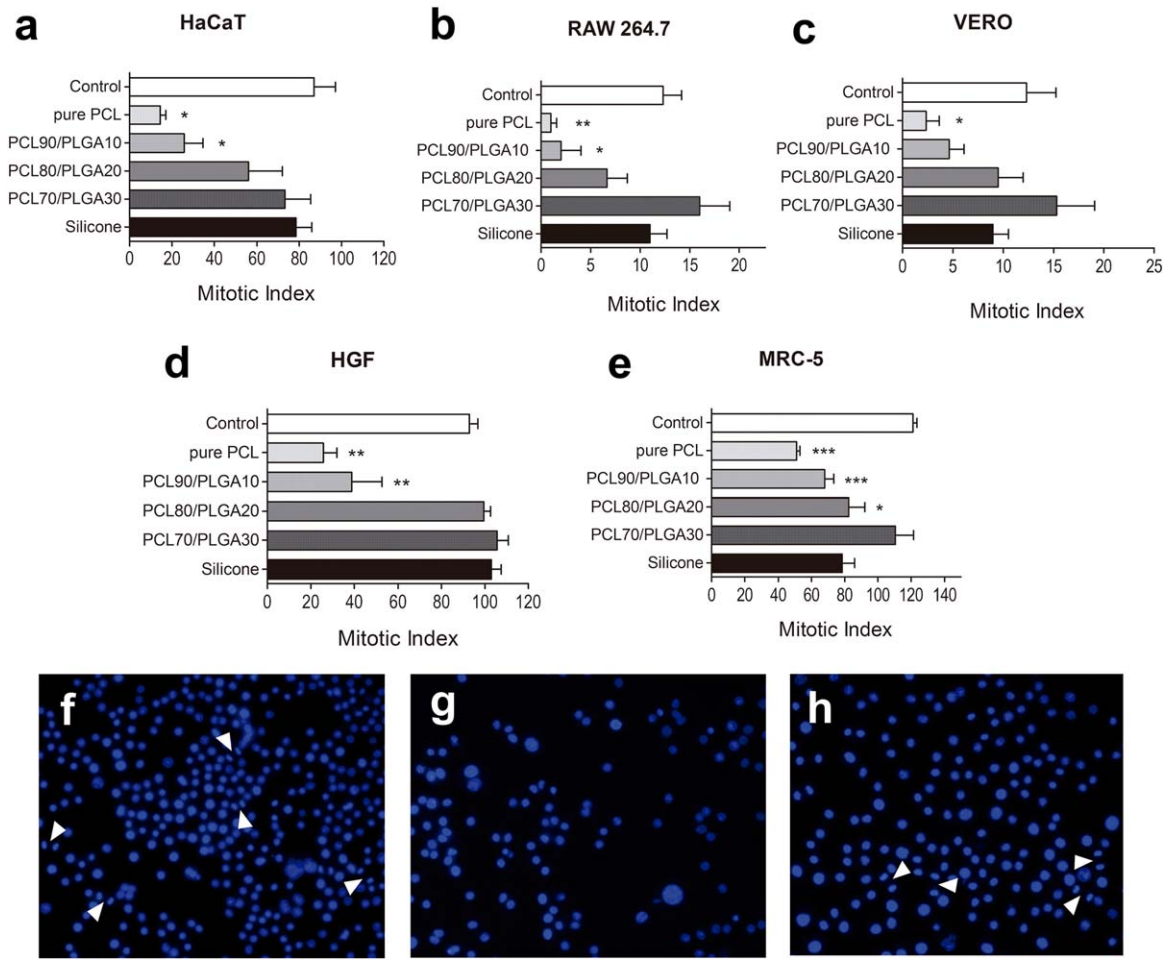

FIGURE 6. Frequency of mitotic cells as a parameter of cell proliferation after 24 h of incubation with smooth membranes. The mitotic index was established for (a) HaCaT, (b) RAW 264.7, (c) VERO, (d) HGF, and (e) MRC-5 cell lines. The blend PCL70/PLGA30 preserved the proliferation capacity for all cell lines tested. Representative images of RAW 264.7 cells showing mitotic figures (white arrows) for cells on (f) control (g) pure PCL and (h) PCL70/PLGA30. $*p < 0.05$, $**p < 0.001$, $***p < 0.0001$ versus control, One-way ANOVA with Tukey *post hoc* test, ($n = 3$).

growth of regenerating axons compared to cells cultured on glass coverslips, which presented random axonal growth (Fig. 9). No apparent difference was noted in axonal orientation of neurons between 15- and 20-μm grooves (Fig. 9).

DISCUSSION

Polyester-based biomaterials are an interesting choice for the fabrication of devices for biological applications since they are biocompatible and biodegradable. These materials have been extensively studied, and some of them were approved by the FDA.[41] Among other approaches, blends have been tested to combine individual characteristics of each polymer, aiming to achieve favorable biological properties.[20,38,42] In the present study, we tested blends of PCL with increasing proportions of PLGA to evaluate their role in cytotoxicity, proliferation and adhesion of cells as well as the capacity of microgrooved membranes to promote cell orientation *in vitro*.

Since PLGA degradation occurs faster than PCL, it potentially increases membrane microporous.[20] Our results showed that degradation did not differ among groups during a 90-day period, suggesting that degradation of PLGA was not enough to cause evident mass loss. The long-term *in vivo* stability of biomaterials is desired. Depending on the extension and severity of the injury, the regeneration and maturation process can take months or even years to fully complete.[43,44] Thus, if used for nerve regeneration, the polymeric systems proposed for conduit preparation should remain intact until complete regeneration is achieved.

It is reported that the average rate of axonal regeneration in humans varies from 1 to 2 mm per day. Therefore, polymeric blends are good choices for the production of new scaffolds for medical applications devoted to slow regenerative processes. One of the advantages of working with blends is the possibility of modulating the degrading time by the combination of different polymers. Considering that the time for complete nerve regeneration depends on the complexity of lesions, the biodegradable polymers and blends proposed in this study are interesting candidates for cases where regenerative process is slow.[43,44]

Proteins present in serum adsorb onto the material surfaces allowing the interaction and binding of cell

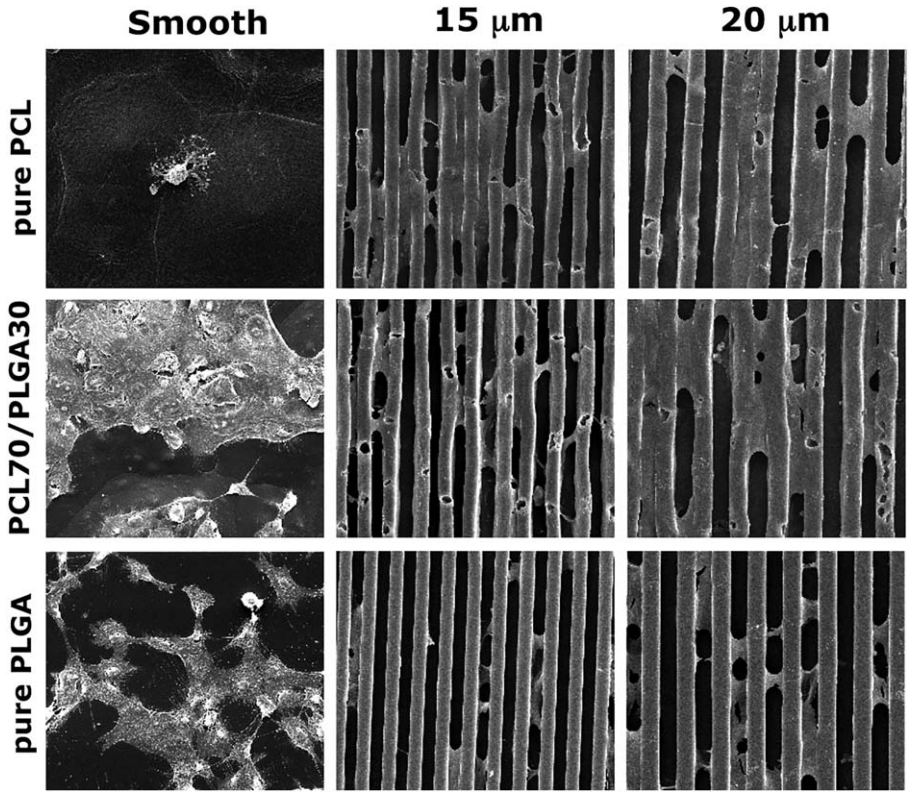

FIGURE 7. SEM of the HGF cells on membranes. Cells attached to the membrane surface of smooth or inside microgrooves of both 15 μm and 20 μm remained adhered to the pure PLGA and PCL70/PLGA30 membranes after 3 days. Few cells remained adhered to the surface of smooth pure PCL membranes compared to the membranes of 15 μm and 20 μm grooves. Original magnification ×1000.

receptors to these proteins, which favors cell attachment and spread to the membrane surface.[45] Different surface properties influence the adsorption of serum proteins to the material, such as chemical composition, hydrophilicity and morphology in nanometric-scale.[42,45,46] The analysis of surface topology showed an increase in the roughness of both pure PLGA and the PCL70/PLGA30 membranes compared to other groups. Increased roughness implies into more proteins adsorbed to the biomaterial surfaces.[46] This hypothesis explains the increased capacity of fibroblasts to adhere to pure PLGA and the PCL70/PLGA30 smooth membranes, as observed either by the SEM or fluorescence microscopy results. The literature shows that hydrophilic surfaces facilitates adhesion and proliferation of cells on the scaffolds.[47–49] The sharp changes in topology and surface roughness can have a direct effect on contact angles, as well as cell—surface interactions of the scaffolds.[50,51] Despite the slight increase in the contact angle found for PLGA membranes, this does not completely explain the good results found for the PCL70/PLGA30 blend. Furthermore, all the membranes were classified as hydrophilic. The increase of PLGA incorporation to 30% (w/w) preserved the viability of the cell lines as well as their proliferation capacity in comparison to pure PCL, being similar to pure PLGA. These results are in agreement with previous studies.[10,19,20,39,52] Conversely, the favorable results presented by the blend PCL70/PLGA30 correlate with high surface roughness presented by this membrane, since the literature has attributed the improvements in cell proliferation to topographic cues promoted by surface roughness.[53,54]

Considering the mechanical properties, pure PCL is a more flexible and suitable material for scaffold preparation compared to PLGA. However, PCL has less affinity for the cells and the blend of the two polymers may result in a material with biological and mechanical advantages.[13,55] In this work, the mixture of the two polymers resulted in a less flexible material when compared to pure PCL, but no statistically significant differences were observed, irrespective of the PLGA concentration.

The use of tubular structures to guide the regrowth of transected nerves has been proven as an efficient alternative to nerve autografts. Nerve conduits produced from biodegradable materials are preferred since they can be produced in large-scale and a second surgery for conduit removal is not required.[28] The natural process of nerve regeneration involves the demyelination and proliferation of Schwann cells at the injury site, as a component of Wallerian degeneration. These cells align longitudinally to the axon growth direction and form the bands of Büngner that are responsible for neuron guiding and orientation.[30] Previous studies have shown that cells respond to surface topographical features.[23,29–32]

The introduction of grooves on membrane surfaces has been efficiently used to improve cell guiding.[23,29,30,32,51] Cell

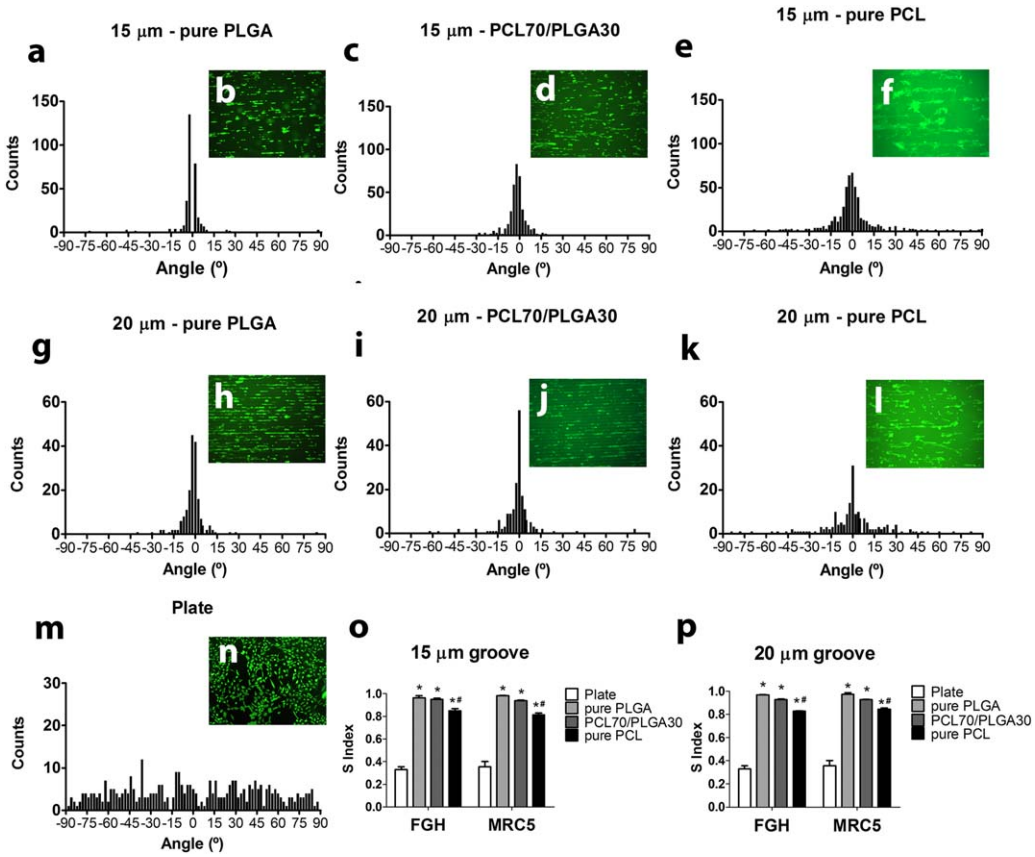

FIGURE 8. Cell morphology and orientation on microgrooved membranes. Fibroblasts were cultured for 3 days on pure PGLA (a,b,g,h), PCL70/PLGA30 (c,d,i,j), pure PCL (e,f,k,l) and tissue-culture plate (m,n). The angle deviations (a,c,e,g,i,k,m) and the respective morphology after fluorescein diacetate staining (b,d,f,h,j,l,n) are plotted for each group. The *S* index was compared among groups for HGF and MRC-5 cells (15 μm) (o) and (20 μm) (p). Original magnification ×100. *$p < 0.05$ versus plate and #$p < 0.05$ versus pure PLGA and PCL70/PLGA30, one-way ANOVA followed by Tukey *post hoc* test ($n = 3$).

orientation was observed for DRG neurons on microgrooved poly(D-lactic acid) membranes and the coculture with Schwann cells improved neurite growth and orientation[31]. Similar results were observed for glioma and Schwann cells on microgrooved membranes of chitosan/polylactic acid at the proportion of 1:10[23] and on laminin-coated membranes.[30,32] The width and depth of grooves also influence cell fate orientation and alignment.[22,30,32,56] Grooves widths between 10 and 20 μm were found to be optimal to promote cell orientation. Grooves with <10 μm-width do not allow cells to enter the groove and larger than 20 μm do not promote cell alignment.[29] We produced 15- and 20-μm width grooves and both of them were able to promote cell orientation, corroborating the results found by other studies. Similarly, grooves with <1.5–2 μm in depth did not promote cell orientation.[30,32,56] Furthermore, membranes easily lose microgrooving due to polymer degradation.[32] For that reasons, we decided to produce membranes with deeper grooves (25-μm height) that efficiently allowed cells to enter into the groove. Additionally, the use of slow degradation polymer blends might contribute to prolonging the degradation time of the grooves, preventing the orientation loss during the regeneration process. Other cell types were also found to become oriented in microgrooved membranes, such as rat mesenchymal stem cells differentiated to Schwann cells[57] and muscle precursor cells.[58] We have used a heterogeneous population of neurons, satellite cells and Schwann cells isolated from DRG for culturing on the membranes. Similar results observed between pure PCL, pure PLGA and PCL70/PLGA membranes in promoting cell adhesion and axon outgrowth might be explained by the surface coating with Geltrex. Despite that, irrespective of the polymeric composition, the topographical cues of the grooves efficiently promoted the axonal guidance of neuron cells corroborating the results obtained for fibroblasts.

The *in vivo* application of microporous and microgrooved PLA conduits promoted myelination and neovascularization of sciatic nerve, improving functional recovery of rats.[59] Promising results were also obtained with microgrooved PCL/PLA conduits with functional recovery similar to nerve autograft.[22] Despite the encouraging outcomes from preclinical studies, no commercially available conduits for clinical applications present these intraluminal microstructures.[41]

In this study, scaffolds of PCL, PLGA and PCL/PLGA blends with and without microgrooves surface were fabricated using solvent casting technique. The PLGA incorporation increased the biological compatibility and surface

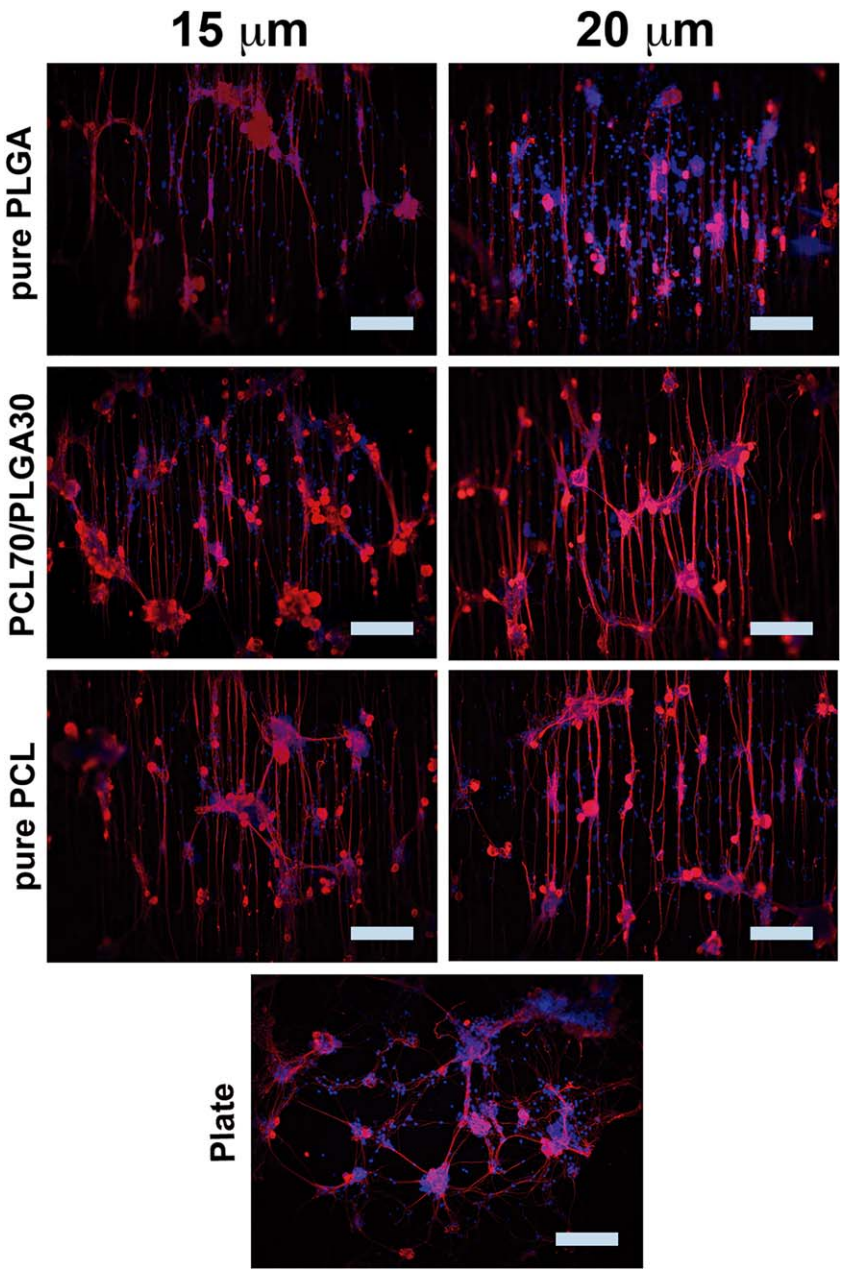

FIGURE 9. Cell morphology and orientation of dorsal root ganglia-derived B-III-tubulin positive neurons growing on 15 and 20 μm microgrooved membranes. The DRG cells were cultured for 3 days on pure PGLA, PCL70/PLGA30, pure PCL membranes and glass coverslips (used as control). Original magnification ×1000; scale bar: 200 μm.

roughness of PCL membranes and it correlates with the increased viability and attachment of cells. The microgrooved PCL70/PLGA30 membranes promoted fibroblast orientation similar to pure PLGA and better that pure PCL and no obvious difference in cell orientation was observed between PCL70/PLGA30 and the pure membranes. Our study brings novel data indicating a favorable profile for PCL70/PLGA30 membranes to promote cell growth, proliferation, and orientation. The microstructuration of membrane surface can be used as a potential option to produce conduits or other devices to guide cell orientation. *In vivo* studies are in progress to evaluate the therapeutic properties of PCL70/PLGA30 membranes in peripheral nerve regeneration models.

CONFLICT OF INTEREST

The authors declare no conflict of interest related to this manuscript.

REFERENCES

1. Limongi T, Tirinato L, Pagliari F, Giugni A, Allione M, Perozziello G, Candeloro P, Di Fabrizio E. Fabrication and applications of micro/nanostructured devices for tissue engineering. Nano-Micro Lett 2017;9:13.

2. Keane TJ, Badylak SF. Biomaterials for tissue engineering applications. Semin Pediatr Surg 2014; 23:112–118.
3. Stratton S, Shelke NB, Hoshino K, Rudraiah S, Kumbar SG. Bioactive polymeric scaffolds for tissue engineering. Bioact Mater 2016;1:93–108.
4. Mundargi RC, Babu VR, Rangaswamy V, Patel P, Aminabhavi TM. Nano/micro technologies for delivering macromolecular therapeutics using poly(d,l-lactide-co-glycolide) and its derivatives. J Control Release 2008;125:193–209.
5. Arslantunali D, Dursun T, Yucel D, Hasirci N, Hasirci V. Peripheral nerve conduits: Technology update. Med Devices 2014;7:405–424.
6. Place ES, Evans ND, Stevens MM. Complexity in biomaterials for tissue engineering. Nat Mater 2009;8:457–470.
7. Sadtler K, Singh A, Wolf MT, Wang X, Pardoll DM, Elisseeff JH. Design, clinical translation and immunological response of biomaterials in regenerative medicine. Nat Rev Mater 2016;1:16040.
8. Daly W, Yao L, Zeugolis D, Windebank A, Pandit A. A biomaterials approach to peripheral nerve regeneration: bridging the peripheral nerve gap and enhancing functional recovery. J R Soc Interface 2012;9:202–221.
9. Pan Z, Ding J. Poly(lactide-co-glycolide) porous scaffolds for tissue engineering and regenerative medicine. Interface Focus 2012; 2:366–377.
10. Hiep NT, Lee BT. Electro-spinning of PLGA/PCL blends for tissue engineering and their biocompatibility. J Mater Sci Mater Med 2010;21:1969–1978.
11. Yoo HS, Kim TG, Park TG. Surface-functionalized electrospun nanofibers for tissue engineering and drug delivery. Adv Drug Deliv Rev 2009;61:1033–1042.
12. Gerzson AdS, Machado DC, da Silva RR, Valente CA, Pagnoncelli RM. Assessment of the viability of NIH3T3 fibroblast cells cultured in polymer matrices with rhGH. J Polym Environ 2017;1–7.
13. Won J-Y, Park CY, Bae JH, Ahn G, Kim C, Lim DH, Cho DW, Yun WS, Shim JH, Huh JB. Evaluation of 3D printed PCL/PLGA/beta-TCP versus collagen membranes for guided bone regeneration in a beagle implant model. Biomed Mater 2016;11:055013.
14. Cho DID, Yoo HJ. Microfabrication methods for biodegradable polymeric carriers for drug delivery system applications: A review. J Microelectromech Syst 2015;24:10–18.
15. Li D, Sun HF, Hu XH, Lin YL, Xu B. Facile method to prepare PLGA/hydroxyapatite composite scaffold for bone tissue engineering. Mater Technol 2013;28:316–323.
16. Park SC, Oh SH, Seo TB, Namgung U, Kim JM, Lee JH. Ultrasound-stimulated peripheral nerve regeneration within asymmetrically porous PLGA/Pluronic F127 nerve guide conduit. J Biomed Mater Res B 2010;94:359–366.
17. Díaz E, Sandonis I, Valle MB. In vitro degradation of poly(caprolactone)/nHA composites. J Nanomater 2014;2014:1.
18. Tang Z, Rhodes N, Hunt J. Control of the domain microstructures of PLGA and PCL binary systems: importance of morphology in controlled drug release. Chem Eng Res Des 2007;85:1044–1050.
19. Tang ZG, Callaghan JT, Hunt JA. The physical properties and response of osteoblasts to solution cast films of PLGA doped polycaprolactone. Biomaterials 2005;26:6618–6624.
20. Tang ZG, Hunt JA. The effect of PLGA doping of polycaprolactone films on the control of osteoblast adhesion and proliferation in vitro. Biomaterials 2006;27:4409–4418.
21. Shen H, Zhang L, Liu M, Zhang Z. Biomedical applications of graphene. Theranostics 2012;2:283–294.
22. Mobasseri A, Faroni A, Minogue BM, Downes S, Terenghi G, Reid AJ. Polymer scaffolds with preferential parallel grooves enhance nerve regeneration. Tissue Eng A 2015;21:1152–1162.
23. Hsu SH, Lu PS, Ni HC, Su CH. Fabrication and evaluation of microgrooved polymers as peripheral nerve conduits. Biomed Microdevices 2007;9:665–674.
24. Simitzi C, Ranella A, Stratakis E. Controlling the morphology and outgrowth of nerve and neuroglial cells: The effect of surface topography. Acta Biomater 2017;51:21–52.
25. Cui L, Li J, Long Y, Hu M, Li J, Lei Z, Wang H, Huang R, Li X. Vascularization of {LBL} structured nanofibrous matrices with endothelial cells for tissue regeneration. RSC Adv 2017;7:11462–11477.
26. Yang J, Wan Y, Tu C, Cai Q, Bei J, Wang S. Enhancing the cell affinity of macroporous poly (L-lactide) cell scaffold by a convenient surface modification method. Polym Int 2003;52:1892–1899.
27. Mobasseri SA, Terenghi G, Downes S. Micro-structural geometry of thin films intended for the inner lumen of nerve conduits affects nerve repair. J Mater Sci Mater Med 2013;24:1639–1647.
28. Pfister LA, Papaloïzos M, Merkle HP, Gander B. Nerve conduits and growth factor delivery in peripheral nerve repair. J Peripher Nerv Syst 2007;12:65–82.
29. Miller C, Shanks H, Witt A, Rutkowski G, Mallapragada S. Oriented Schwann cell growth on micropatterned biodegradable polymer substrates. Biomaterials 2001;22:1263–1269.
30. Hsu SH, Chen CY, Lu PS, Lai CS, Chen CJ. Oriented Schwann cell growth on microgrooved surfaces. Biotechnol Bioeng 2005;92: 579–588.
31. Miller C, Jeftinija S, Mallapragada SK. Micropatterned Schwann cell-seeded biodegradable polymer substrates significantly enhance neurite alignment and outgrowth. Tissue Eng 2001;7:705–715.
32. Miller C, Jeftinija S, Al MET. Synergistic effects of physical and chemical guidance cues on neurite alignment and outgrowth on biodegradable polymer substrates. Tissue Eng 2002;8:367–378.
33. F1635-11, A. Standard Test Method for in vitro Degradation Testing of Hydrolytically Degradable Polymer Resins and Fabricated Forms for Surgical Implants (2011).
34. American A, Standard N. Standard Test Method for Tensile Properties of Thin Plastic Sheeting 1. 2002;14:1–11.
35. ISO 10993-5:2009. Biological Evaluation of Medical Devices—Part 5: Tests for In Vitro Cytotoxicity. Geneva Switzerland: International Organization for Standardization; 2009;1–34.
36. Sperling LE, Reis KP, Pozzobon LG, Girardi CS, Pranke P. Influence of random and oriented electrospun fibrous poly(lactic-co-glycolic acid) scaffolds on neural differentiation of mouse embryonic stem cells. J Biomed Mater Res A 2017;105:1333–1345.
37. Barbanti SH, Santos AR, Zavaglia AC, Duek EAR. Poly (e-caprolactone) and poly (D,L-lactic acid-co-glycolic acid) scaffolds used in bone tissue engineering prepared by melt compression—Particulate leaching method. J Mater Sci Mater Med 2011;22:2377–2385.
38. Gaona LA, Gómez Ribelles JL, Perilla JE, Lebourg M. Hydrolytic degradation of PLLA/PCL microporous membranes prepared by freeze extraction. Polym Degrad Stab 2012;97:1621–1632.
39. Duarte MAT, Duek EAR, Motta AC. In Vitro Degradation of poly (L-co-D,L lactic acid) containing PCL-T. Polímeros 2014;24:1–8.
40. Hoornaert A, d'Arros C, Heymann M-F, Layrolle P. Biocompatibility, resorption and biofunctionality of a new synthetic biodegradable membrane for guided bone regeneration. Biomed Mater 2016;11:045012.
41. Kehoe S, Zhang XF, Boyd D. FDA approved guidance conduits and wraps for peripheral nerve injury: A review of materials and efficacy. Injury 2012;43:553–572.
42. Sun M, Kingham PJ, Reid AJ, Armstrong SJ, Terenghi G, Downes S. In vitro and in vivo testing of novel ultrathin PCL and PCL/PLA blend films as peripheral nerve conduit. J Biomed Mater Res - Part A 2010;93:1470–1481.
43. Griffin M, Malahias M, Hindocha S, Wasim KS. Peripheral nerve injury: Principles for repair and regeneration. Open Orthop J 2014;8:199–203.
44. Grinsell D, Keating CP. Peripheral nerve reconstruction after Injury: A review of clinical and experimental therapies. Biomed Res Int 2014; 2014:1.
45. Elbert DL, Hubbell JA. Surface treatments of polymers for biocompatibility. Annu Rev Mater Sci 1996;26:365–394.
46. Scopelliti PE, Borgonovo A, Indrieri M, Giorgetti L, Bongiorno G, Carbone R, Podestà A, Milani P. The effect of surface nanometre-scale morphology on protein adsorption. PLoS One 2010;5: e11862–e11869.
47. Chen W, Shao Y, Li X, Zhao G, Fu J. Nanotopographical surfaces for stem cell fate control: Engineering mechanobiology from the bottom. Nano Today 2014;9:759–784.
48. Jing X, Mi H, Wang X, Peng X, Turng L. Shish–Kebab structured poly (e-caprolactone) nanofibers hierarchically decorated with chitosan—Poly (e-caprolactone) copolymers for bone tissue engineering. ACS Appl Mater Interfaces 2015;7:6955–6965.
49. Zhang F, Qian Y, Chen H, Xu Y, Yang J, Zhou X, Gu N. The preosteoblast response of electrospinning PLGA/PCL nanofibers: Effects of biomimetic architecture and collagen I. Int J Nanomed 2016;11: 4157–4171.

50. Croll TI, Connor AJO, Stevens GW, Cooper-white JJ. Controllable surface modification of Poly (lactic-co-glycolic acid) (PLGA) by hydrolysis or aminolysis I: Physical, chemical, and theoretical aspects. Biomacromolecules 2004;5:463–473.
51. Cai K, Yao K, Cui Y, Yang Z, Li X, Xie H, Qing T, Gao L. Influence of different surface modification treatments on poly (d, l -lactic acid) with silk fibroin and their effects on the culture of osteoblast in vitro. Biomaterials 2002;23:1603–1611.
52. Ouyang HW, Goh JCH, Mo XM, Teoh SH, Lee EH. Characterization of anterior cruciate ligament cells and bone marrow stromal cells on various biodegradable polymeric films. Mater Sci Eng C 2002;20:63–69.
53. Díaz E, Puerto I, Ribeiro S, Lanceros-Mendez S, Barandiarán JM. The influence of copolymer composition on PLGA/nHA scaffolds' cytotoxicity and in vitro degradation. Nanomaterials 2017;7:173.
54. Balint R, Cassidy NJ, Cartmell SH. Conductive polymers: Towards a smart biomaterial for tissue engineering. Acta Biomater 2014; 10:2341–2353.
55. Shim J-H, Huh JB, Park JY, Jeon YC, Kang SS, Kim JY, Rhie JW, Cho DW. Fabrication of blended polycaprolactone/poly (lactic-co-glycolic acid)/β-tricalcium phosphate thin membrane using solid freeform fabrication technology for guided bone regeneration. Tissue Eng Part A 2013;19:317–328.
56. Chua JS, Chng CP, Moe AA, Tann JY, Goh EL, Chiam KH, Yim EK. Extending neurites sense the depth of the underlying topography during neuronal differentiation and contact guidance. Biomaterials 2014;35:7750–7761.
57. Sharma AD, Zbarska S, Petersen EM, Marti ME, Mallapragada SK, Sakaguchi DS. Oriented growth and transdifferentiation of mesenchymal stem cells towards a Schwann cell fate on micropatterned substrates. J Biosci Bioeng 2016; 121:325–335.
58. Flaibani M, Boldrin L, Cimetta E, Piccoli M, De Coppi P, Elvassore N. Muscle differentiation and myotubes alignment is influenced by micropatterned surfaces and exogenous electrical stimulation. Tissue Eng Part A 2009;15:2447–2457.
59. Hsu S, Ni H. Fabrication of the microgrooved/microporous polylactide substrates as peripheral nerve conduits and in vivo evaluation. Tissue Eng Part A 2009;15:1381–1390.